

**A MATHEMATICAL MODEL DEVELOPMENT FOR THE
QUASI-STATIC LATERAL COLLAPSE OF THE GENERALISED
GEOMETRIC HOLLOW SHAPES**

MUHAMAD GHAZALI BIN KAMARDAN

Thesis Submitted to the Centre for Graduate Studies, Universiti Pertahanan Nasional
Malaysia, in Fulfilment of the Requirements for the Degree of Doctor of Philosophy

September 2014

ABSTRACT

The purpose of this research is to develop a general predictive **mathematical** model of the deformation behaviours for various symmetric geometrical tubes under lateral compression between two flat rigid plates. The mathematical model has been proposed based on rigid, perfectly plastic model and the energy balance method. The mathematical models are divided into two cases i.e. 'Case 1' and 'Case 2' based on the geometrical shapes of the tubes. 'Case 1' is for shapes with number of sides 6, 10, 14 and so on such as hexagonal, decagonal and tetra-decagonal tubes. Whereas, 'Case 2' is for shapes with number of sides 4, 8, 12 and so on such as square, octagonal and dodecagonal tubes. The prediction or assumption used in this mathematical model was that the tubes would deform in phase by phase during plastic deformation. In order to achieve this purpose, the deformation behaviour and the energy-absorption performance of various geometrical tube shapes need to be determined. The geometrical tubes shapes which were studied include square, hexagonal, octagonal, decagonal, dodecagonal and tetra-decagonal tubes. For that, experimental tests and finite element analysis (FEA) simulation were conducted to determine the collapse behaviour of these various symmetrical geometric tubes. First, the quasi-static lateral compression test was conducted on square and cylindrical tubes experimentally and by FEA simulation method by using INSTRON Universal Testing Machine and ABAQUS software respectively. Both results were compared to validate the FEA simulation results. Then, the validated FEA simulation method was performed for these various symmetrical geometric tubes to determine their deformation behaviour

and energy-absorption performance and then to validate the newly mathematical model. The comparison between the experiment and FEA simulation had shown good agreement. The simulation study showed that square and symmetric hexagonal tubes deformed with 1 phase of plastic deformation, symmetric octagonal and decagonal tubes deformed with 2 phases of plastic deformation, symmetric dodecagonal and tetra-decagonal tubes deformed with 3 phases of plastic deformation. It was determined that, the general mathematical model had succeeded to predict the deformation behaviour of various symmetric geometrical shapes for both cases but discrepancy occurred for certain specimens due to sudden high peak at the last phase and small angle difference for neighbouring sides. The energy – absorption performance analyses for different types of symmetric geometrical tubes had shown that symmetric hexagonal tube produced the best energy-absorption with high total energy absorption, low yield stress and long stroke without any sudden jump force.

ABSTRAK

Tujuan kajian ini adalah untuk membangunkan model matematik ramalan umum bagi tingkah laku ubahan-bentuk untuk berbagai tiub bergeometrik simetri di bawah mampatan sisian antara dua plat tegar rata. Model matematik dicadangkan berdasarkan model tegar, plastik sempurna dan kaedah tenaga saksama. Model matematik ini terbahagi kepada dua kes iaitu 'Kes 1' dan 'Kes 2' berdasarkan kepada bentuk geometrik tiub. Kes '1' adalah untuk bentuk tiub dengan bilangan sisi 6, 10, 14 dan seterusnya seperti tiub heksagon, dekagon dan tetra-dekagon. Manakala, 'Kes 2' bagi bentuk tiub dengan bilangan sisi 4, 8, 12 dan seterusnya seperti tiub segi empat sama, oktagon dan dodekagon. Ramalan atau andaian yang digunakan dalam model matematik ini adalah bahawa tiub akan mengalami ubah-bentuk fasa demi fasa semasa ubahan-bentuk plastik. Untuk mencapai tujuan ini, tingkah-laku ubah-bentuk dan prestasi serapan-tenaga tiub-tiub berbagai bentuk geometrik perlu ditentukan. Bentuk-bentuk geometrik tiub yang dikaji termasuk tiub segi empat sama, heksagon, oktagon, dekagon, dodekagon dan tetra-dekagon. Untuk itu, simulasi analisis unsur terhingga (FEA) dan ujian eksperimen telah dijalankan untuk menentukan tingkah-laku keruntuhan tiub-tiub bergeometrik simetri tersebut. Pertama, ujian mampatan sisian separa statik dijalankan ke atas tiub segi empat sama dan tiub silinder secara eksperimen menggunakan mesin ujikaji universal INSTRON dan secara simulasi FEA menggunakan perisian ABAQUS. Kedua-dua keputusan dibandingkan untuk mengesahkan keputusan simulasi FEA. Kemudian, kaedah simulasi FEA yang telah disahkan dilakukan ke atas kesemua tiub-tiub bergeometrik

simetri tersebut untuk menentukan tingkah laku ubahan-bentuk dan prestasi serapan-tenaga bentuk-bentuk tersebut dan kemudian untuk mengesahkan model baru matematik. Perbandingan antara eksperimen dan simulasi FEA telah menunjukkan perjanjian yang baik. Kajian simulasi menunjukkan bahawa tiub segiempat sama dan tiub heksagon simetri mengalami ubah-bentuk dengan 1 fasa pada ubahan-bentuk plastik, tiub oktagon simetri dan tiub dekaagon simetri mengalami ubah-bentuk dengan 2 fasa pada ubahan-bentuk plastik, tiub dodekaagon simetri dan tiub tetradekaagon simetri mengalami ubah-bentuk dengan 3 fasa pada ubahan-bentuk plastik. Telah dipastikan bahawa model matematik umum telah berjaya untuk meramalkan tingkah-laku ubahan-bentuk pelbagai bentuk tiub bergeometrik simetri bagi kedua-dua kes. Walau bagaimanapun, berlaku percanggahan pada spesimen tertentu disebabkan kemunculan puncak tinggi secara mendadak di fasa terakhir dan perbezaan sudut yang kecil pada sisi-sisi yang berjiran. Analisis prestasi serapan-tenaga pada tiub-tiub bergeometrik simetri yang berbeza telah menunjukkan bahawa tiub heksagon simetri menghasilkan serapan-tenaga terbaik dengan jumlah serapan-tenaga yang tinggi, kadar hasil yang rendah dan strok yang panjang tanpa mana-mana peningkatan mendadak pada kuasa.

ACKNOWLEDGEMENTS

All the praises belong to Allah, The Lord of the universe who has given the author the strength and ability to pursue and complete his PhD. The author would like to acknowledge the Ministry of Higher Education of Malaysia and Universiti Tun Hussein Onn Malaysia for sponsoring his PhD endeavour.

The author wishes to express his sincere gratitude to all his supervisors Prof. Dr. Ahmad Mujahid bin Ahmad Zaidi, Prof. Dato' Dr. Mohd. Noh bin Dalimin and Dr. Mohd Zaid bin Othman for their enthusiastic guidance, time, support, encouragement and comments in developing and completing this thesis. The author also would like to express his gratitude to SIRIM berhad, Malaysia which provided the facilities for the FEA simulation analysis via ABAQUS software.

The author is indebted to these individuals who have directly or indirectly assisted him throughout his studies:

Late Mr. Ezkandar Sanny bin Jailani who had given him courage and support; Dr. Waluyo and Mr. Ahmad bin Abbas for helping the author with the 'ABAQUS'FEA simulation; Mr. Yaakob, Mr. Faizal, Mr. Adam and Mr. Shafik for their help in the experimental work; Mr. Mahmud, Mr. Zulhafni, and Mr. Kana for their helpful discussion and suggestion in impact related areas; Assoc. Prof. Rozaini, Mr. Nazib, Mr. Daniel, Mr. Joseph, Mr. Zulkarnain and Mr. Kamarul Affendi for their support in general areas of the studies, and Mr. Zainal for proofreading the completed thesis. Last but not least, the author would also like to express his appreciation to Assoc. Prof. Dr. Azmi bin Khamis and Prof. Dr. Hashim bin Saim whom made this post graduate study possible.

APPROVAL

This thesis was submitted to the Senate of Universiti Pertahanan Nasional Malaysia and has been accepted as fulfilment of the requirements for the degree of Doctor of Philosophy. The members of the Supervisory Committee were as follows:

Ahmad Mujahid Bin Ahmad Zaidi, PhD
Professor
Faculty of Engineering
Universiti Pertahanan Nasional Malaysia
(Chairman)

Mohd Noh Bin Dalimin, PhD
Professor/ Dato'
Office of the Vice-Chancellor / Chancellery Office
Universiti Tun Hussein Onn Malaysia
(Member)

Mohd Zaid Bin Othman, PhD
Faculty of Engineering
Universiti Pertahanan Nasional Malaysia
(Member)

TABLE OF CONTENTS

	Page
ABSTRACT	ii
ABSTRAK	iv
ACKNOWLEDGEMENTS	vi
APPROVAL	vii
DECLARATION	viii
LIST OF TABLES	xii
LIST OF FIGURES	xiii
LIST OF ABBREVIATIONS	xxi
CHAPTER	
1 INTRODUCTION	1
1.1 Background of the Research	1
1.2 The Crashworthiness Properties and the Energy-absorption System	3
1.3 Problem Statements	4
1.4 Research Objectives	5
1.5 Scope of Research	5
1.6 Layout of the Thesis	6
2 LITERATURE REVIEW	9
2.1 Introduction	9
2.2 Axial Compression	14
2.2.1 Circular Tube	17
2.2.2 Square Tube	19
2.2.3 Hexagonal Tube	23
2.2.4 Frusta Tubes	24
2.2.5 Other Shape Tubes	25
2.2.6 Multi-cell Tubes	25
2.2.7 Inversion of Tubes	26
2.2.8 Splitting Tubes	28
2.3 Lateral Compression	30
2.3.1 Cylindrical Tube	33
2.3.2 Square Tube	34
2.3.3 Hexagonal Tube	35
2.3.4 Oblong Tube	36
2.3.5 Ring System Tubes	38
2.3.6 Nested Cylindrical System	40
2.3.7 Constrained Cylindrical Tubes	43
2.3.8 Other Cylindrical Systems	46
2.4 Fundamentals of the Mathematical Model	48
2.4.1 The Bending Moment and the Curvature of Central Axis	53

2.4.2	Statically Admissible Stress Field and Lower Bound Theorem	55
2.4.3	Kinematically Admissible Velocity/Displacement Field and Upper Bound Theorem	56
2.4.4	Lateral Collapse of Symmetric Geometrical Tubes	57
3	METHODOLOGY	60
3.1	Introduction	60
3.2	The Experimental Procedures	65
3.2.1	Specimen Specifications	65
3.2.2	Material Properties	66
3.2.3	The Experimental Test Samples	68
3.2.4	The Tensile Test Results	74
3.2.5	Quasi-Static Compressive Test	74
4	FINITE ELEMENT ANALYSIS	77
4.1	Introduction	77
4.2	The Geometrical Shapes	78
4.2.1	Square and Symmetric Hexagonal Tubes	79
4.2.2	Symmetric Octagonal Tube	81
4.2.3	Symmetric Decagonal (Polygon with Ten Sides) Tubes	83
4.2.4	Symmetric Dodecagonal and Tetra-decagonal Tubes	84
4.3	The Development of the Finite Element Analysis Model	87
4.3.1	The Parts Module	88
4.3.2	The Material Property Module	89
4.3.3	The Assemble Module	90
4.3.4	The Step Module	91
4.3.5	The interaction Module	92
4.3.6	The Load Module (Load and Boundary Condition)	93
4.3.7	The Mesh Module	94
5	MATHEMATICAL MODEL	95
5.1	Introduction	95
5.2	'Case 1'	96
5.2.1	Hexagon	97
5.2.2	Decagon (Polygon with Ten Sides)	102
5.2.3	Tetra-decagon (Polygon with Fourteen Sides)	110
5.2.4	The Generalized Mathematical Model for 'Case 1'	115
5.3	'Case 2'	121
5.3.1	Square	121
5.3.2	Octagon	123
5.3.3	Dodecagon (Polygon with Twelve Sides)	126
5.3.4	The Generalized Mathematical Model for 'Case 2'	128
5.4	The Load-Deformation Behaviour	132

6	RESULTS AND DISCUSSION	134
6.1	Introduction	134
6.2	Validation of Simulation Results with Experimental Data	137
6.3	Symmetric Hexagonal and Square Tubes	140
6.3.1	Load- Deformation Behaviour of Square and Various Symmetric Hexagonal Tubes Compared with Cylindrical Tube	141
6.3.2	Energy-Absorption Performance	143
6.3.3	Validation of Mathematical Model Results with Simulation Results	145
6.4	Symmetric Octagonal Tubes	148
6.4.1	Load-Deformation Behaviour	148
6.4.2	Energy-Absorption Performance	151
6.4.3	Deformation Mode	152
6.4.4	Validation of Mathematical Model Results with Simulation Results	153
6.5	Symmetric Decagonal (Polygon with Ten Sides) Tubes	156
6.5.1	Load- Deformation Behaviour	156
6.5.2	Energy-Absorption Performance	159
6.5.3	Deformation Mode	161
6.5.4	Validation of Mathematical Model Results with Simulation Results	162
6.6	Symmetric Dodecagonal (Polygon with Twelve Sides) Tubes	166
6.6.1	Load-Deformation Behaviour	166
6.6.2	Energy-Absorption Performance	169
6.6.3	Deformation Mode	170
6.6.4	Validation of Mathematical Model Results with Simulation Results	171
6.7	Symmetric Tetra-decagonal (Polygon with Fourteen Sides) Tubes	174
6.7.1	Load-Deformation Behaviour	175
6.7.2	Energy-Absorption Performance	177
6.7.3	Deformation Mode	179
6.7.4	Validation of Mathematical Model Results with Simulation Results	181
7	CONCLUSIONS AND SUGGESTIONS FOR FUTURE WORK	183
7.1	Conclusions	183
7.2	Suggestions for Future Work	186
	REFERENCES	190
	BIODATA OF THE STUDENT	196
	CURRICULUM VITAE	197
	LIST OF PUBLICATIONS	201

LIST OF TABLES

TABLE NO.	TITLE	PAGE
Table 3.1	The dimensions of the rectangular tension test specimens (ASTM,2004).	70
Table 3.2	The Dimensions of the Large-Diameter Tubular Tension Test Specimens (ASTM, 2004).	73
Table 3.3	The mechanical properties of the aluminium and mild steel tubes obtained from tensile test.	74
Table 4.1	The material mechanical properties of stainless steel.	90
Table 5.1	The polygon used in the mathematical study.	96
Table 5.2	Load-deformation behaviour prediction for various symmetric geometrical tube shapes.	132
Table 6.1	Energy absorption produced by cylindrical, square and various symmetric hexagonal tubes.	143
Table 6.2	Energy absorption produced by various symmetric octagonal tubes.	151
Table 6.3	Energy absorption produced by various symmetric decagonal tubes.	159
Table 6.4	Energy absorption produced by various symmetric dodecagonal tubes.	169
Table 6.5	Energy absorption produced by various symmetric tetra-decagonal tubes.	177

LIST OF FIGURES

FIGURE NO.	TITLE	PAGE
Figure 2.1	Two type of structure before (dotted line) and during compressive loading (a) Type I structure and (b) Type II structure (Calladine and English, 1984).	12
Figure 2.2	Graph of Load-Displacement of Type I and Type II (Calladine and English, 1984).	12
Figure 2.3	Collapse behaviour of tube under lateral compression (a) Strain-hardening behaviour, (b) Strain-softening behaviour and (c) Perfectly-plastic behaviour (Li et al., 2006).	13
Figure 2.4	The assumption of axi-symmetric deformation mechanism (Alexander, 1960).	15
Figure 2.5	An improved axi-symmetric deformation model (Abramowicz and Jones, 1984a, 1986).	16
Figure 2.6	Deformation mechanism for axi-symmetric model with improved arc profile (Grzebieta, 1990).	16
Figure 2.7	Axi-symmetric deformation model of a cylindrical tube (Wierzbicki et al., 1992).	16
Figure 2.8	Various collapse modes for thin-walled circular aluminium tubes under axial loading (a) axisymmetric mode (concertina); (b) non-symmetric mode (diamond) and (c) mixed mode (Guillow et al., 2001)	17
Figure 2.9	The kagome sandwich column's geometrical construction (Zhang et al., 2010).	18
Figure 2.10	Deformation modes of square tube from left to right : One extensional lobe; Two extensional lobes and One extensional lobe and one asymmetric lobe where S = symmetric, E = extensional, A = asymmetric, T = transition (Fyllingen et al., 2012).	20

Figure 2.11	Finite element models of three types of tube: (a) conventional tube without groove; (b) tube with four grooves i.e. one groove on every sidewall; and (c) tube with grooves i.e. one groove on two opposite sidewalls (Zhang and Huh, 2009).	21
Figure 2.12	Origami pattern introduced on square tube (a) side view and (b) top view (Song et al., 2012).	22
Figure 2.13	Final post-buckling deformation state of a hexagonal sectioned model using LS-DYNA (Rossi et al., 2005).	23
Figure 2.14	The diagram of the geometrical structure for the straight and tapered rectangular tubes (Nagel and Thambiratnam, 2005).	24
Figure 2.15	The specimens geometrical cross-sections left to right: hexagon, octagon, 12-sided star and 16-sided star (Fan et al., 2013).	25
Figure 2.16	Section geometry and dimensions of various multi-cell (Nia and Parsapour, 2014).	26
Figure 2.17	Deformed shape diagram of a cylindrical tube under internal inversion loading under experimental test and ABAQUS simulation (Reid and Harrigan, 1998).	27
Figure 2.18	The sketch of the experimental set-up by Huang et al. (2002).	28
Figure 2.19	Typical square metal tube specimen after the performed experimental tests (Huang et al., 2002).	29
Figure 2.20	Schematic diagram of the experimental set-up of blast loading (Kim et al., 2013).	30
Figure 2.21	Theoretical and experimental diagrams of lateral load/length-displacement of the empty steel specimen HSE-05 (Niknejad and Rahmani, 2014).	36
Figure 2.22	Schematic of an oblong sample tube under quasi-static load (Baroutaji et al., (2014).	37
Figure 2.23	Deformation behaviour pattern of brass rings fixed at one end after the impact loading of 34 m/s (Reid and Reddy, 1983).	38

Figure 2.24	The deformation systems of hexagonal rings (Mahdi and Hamouda, 2012).	40
Figure 2.25	The compression of three-tube system at the initial and final stages (Morris et al., 2006).	41
Figure 2.26	A schematic design of both the standard and optimised design of nested oblong tubes systems (Olabi et al., 2008)	42
Figure 2.27	Symmetric and asymmetric deformations of braced metal tubes (Wu and Carney, 1997).	45
Figure 2.28	Two deformation stages for a 20° braced elliptical tube (Wu and Carney, 1998)	46
Figure 2.29	Three types of stress-strain curves (a) the stress remains at yield stress, Y as the deformation continuous, (b) the stress increased linearly as the deformation continues, (c) stress increased by a power law as the deformation continues (Lu and Yu, 2003).	49
Figure 2.30	Three types of idealised stress-strain curves under tension: (a) elastic, perfectly plastic; (b) elastic, linear hardening; and (c) elastic, power hardening (Lu and Yu, 2003).	50
Figure 2.31	Three types of rigid, plastic model stress-strain curves (a) rigid, perfectly plastic, (b) rigid, linear hardening; and (c) rigid, power hardening (Lu and Yu, 2003).	52
Figure 2.32	Bending profile of an elastic, perfectly plastic beam: (a) stress across the thickness; (b) the diagram of non-dimensional moment vs. curvature (Yu and Zhang, 1996).	54
Figure 2.33	Bending profile of a rigid, perfectly plastic beam: (a) stress across the thickness; (b) the diagram of moment vs. curvature (Yu and Zhang, 1996).	55
Figure 3.1	Various tube's geometrical shapes used in this study (a) hexagon, (b) decagon (10 sides), (c) tetra-decagon (14 sides), (d) square, (e) octagon and (f) dodecagon (12 sides)	61
Figure 3.2	Flow-chart of the research methodology	64
Figure 3.3	Samples of the metallic symmetric tube specimens: (a) Aluminium square tube, (b) Mild steel cylindrical tube	66

Figure 3.4	Tensile test using servo hydraulic dynamic testing machine	67
Figure 3.5	Tensile test using servo hydraulic dynamic testing machine	68
Figure 3.6	CNC vertical milling machine	69
Figure 3.7	The drawing of the rectangular tension test specimens (ASTM, 2004).	70
Figure 3.8	The uniaxial tensile test samples of the square cross section aluminium tube (a) before the tensile test; (b) during the tensile test.	71
Figure 3.9	Cutting off location of a longitudinal tensile test specimens from large-diameter tube (ASTM, 2004).	72
Figure 3.10	The sketch of the large-diameter tubular tensile test specimens (ASTM, 2004).	72
Figure 3.11	The uniaxial tensile test samples of the circular cross section mild steel tube (a) before tensile test; (b) the sample break during tensile test.	73
Figure 3.12	Compression test using the Universal Test Machine	75
Figure 3.13	The shape of the circular tube with 4 stationary hinges.	76
Figure 3.14	The shape of the square tube 6 stationary hinges.	76
Figure 4.1	A square tube: (a) The drawing of hollow square shape; (b) The 3D dimensional diagram of square tube in ABAQUS software.	79
Figure 4.2	Symmetric hexagonal shape	80
Figure 4.3	Hexagonal shapes at various angles, θ (a) 15° , (b) 30° , (c) 45° and (d) 60° .	81
Figure 4.4	Symmetric octagonal shape	81
Figure 4.5	Symmetric octagonal shapes at various angles, θ_1 (a) 30° , (b) 45° and (c) 60° .	82
Figure 4.6	Symmetric decagonal shape	83

Figure 4.7	Symmetric decagonal shapes of $\theta_1 = 45^\circ$ and various angles, θ_2 (a) 15° and (b) 30° .	84
Figure 4.8	Symmetric decagonal shapes of $\theta_1 = 60^\circ$ and various angles, θ_2 (a) 15° , (b) 30° and (c) 45° .	84
Figure 4.9	Symmetric dodecagonal shape	85
Figure 4.10	Symmetric tetra-decagonal shape	85
Figure 4.11	Symmetric dodecagonal shapes of $\theta_1 = 60^\circ$ and various angles, θ_2 (a) 15° , (b) 30° and (c) 45° .	86
Figure 4.12	Hollow symmetric tetra-decagon shapes of $\theta_1 = 60^\circ$, $\theta_2 = 45^\circ$ and Various Angles, θ_3 (a) 15° and (b) 30° .	87
Figure 4.13	The diagram of symmetric hexagonal tube placed in between two rigid plates.	90
Figure 5.1	Symmetric hexagonal shape	97
Figure 5.2	Symmetric hollow hexagon shape compressed between two rigid plates	98
Figure 5.3	The collapse of first quadrant of a symmetric hollow hexagon shape during compression	99
Figure 5.4	The final collapse of first quadrant of a symmetric hollow hexagon shape under lateral compression	101
Figure 5.5	Symmetric decagon shape	103
Figure 5.6	Symmetric hollow decagon shapes compressed between the two rigid plates	104
Figure 5.7	The collapse of first quadrant of a symmetric hollow decagonal shape during 'Phase 1' deformation under lateral compression	105
Figure 5.8	Complete deformation of 'Phase 1' of decagonal tube under lateral compression	106
Figure 5.9	'Phase 2' collapse of symmetric hollow decagon shapes	108

Figure 5.10	Symmetric tetra-decagonal shape	111
Figure 5.11	Shape transformations of symmetric tetra-decagonal tubes	112
Figure 5.12	Generalised symmetric polygonal shape of 'Case 1'	116
Figure 5.13	Square shape	122
Figure 5.14	Symmetric octagonal shape	123
Figure 5.15	Shape transformation of symmetric octagonal tubes	124
Figure 5.16	Symmetric dodecagon shapes	126
Figure 5.17	Shape transformations of symmetric dodecagonal tubes	127
Figure 5.18	Generalised symmetric polygonal shape of 'Case 2'	129
Figure 6.1	The shape's dimension of various symmetric geometrical tubes	137
Figure 6.2	Force vs deflection diagrams - simulation results compared against the experimental data obtained from the lateral loading of tubes (a) Aluminium square tube (b) Mild steel cylindrical tube.	139
Figure 6.3	Square and various hexagon shapes.	140
Figure 6.4	Force vs deformation/ total height relationship for cylindrical, square and various symmetric hexagonal tubes.	141
Figure 6.5	Comparing mathematical against simulation results of force vs deformation/total height relationship of square and symmetrical hexagonal of various angles, θ tubes: (a) square ($\theta = 0^\circ$), (b) 15° , (c) 30° , (d) 45° and (e) 60° .	146
Figure 6.6	Symmetric octagonal shape	148
Figure 6.7	Force vs deformation/ total height relationship of cylindrical and symmetric octagonal of various angles, θ_1 and $\theta_2 = 0^\circ$ tubes.	149
Figure 6.8	Comparing deformation mode results of mathematical against simulation results at 'Phase 1' and 'Phase 2' of symmetric octagonal tubes.	152

Figure 6.9	Comparing mathematical against simulation results of force vs deformation/total height relationship of symmetric octagonal tubes of various angle θ_1 and $\theta_2 = 0^\circ$ (a) 30° , (b) 45° and (c) 60° .	154
Figure 6.10	Symmetric decagonal shapes	156
Figure 6.11	Force vs deformation/ total height relationship of cylindrical and symmetric decagonal of various angles θ_1 and θ_2 tubes.	157
Figure 6.12	Comparing deformation mode results of mathematical against simulation result at 'Phase 1' and 'Phase 2' of symmetric decagonal tubes	162
Figure 6.13	Comparing mathematical against simulation results of force vs deformation/total height relationship of symmetric decagonal tubes of Various θ_1 and θ_2 . (a) $\theta_1 = 45^\circ$, $\theta_2 = 15^\circ$, (b) $\theta_1 = 45^\circ$, $\theta_2 = 30^\circ$, (c) $\theta_1 = 60^\circ$, $\theta_2 = 15^\circ$, (d) $\theta_1 = 60^\circ$, $\theta_2 = 30^\circ$ and (e) $\theta_1 = 60^\circ$, $\theta_2 = 45^\circ$.	164
Figure 6.14	Symmetric dodecagon shapes	166
Figure 6.15	Force vs deformation/ total height relationship of cylindrical and symmetric dodecagonal tubes of $\theta_1 = 60^\circ$, various angles θ_2 and $\theta_3 = 0^\circ$ tubes.	167
Figure 6.16	Comparing deformation mode result of mathematical against simulation result at 'Phase 1', 'Phase 2' and 'Phase 3' of symmetric dodecagonal tubes.	170
Figure 6.17	Comparing mathematical against simulation results of force vs deformation/total height relationship of symmetric dodecagonal tubes of $\theta_1 = 60^\circ$, various angles θ_2 and $\theta_3 = 0^\circ$: (a) 15° , (b) 30° and (c) 45° .	172
Figure 6.18	Symmetric tetra-decagonal shapes	174
Figure 6.19	Force vs deformation/ total height relationship of cylindrical, Dodecagonal- 60-45, Tetra-decagonal-60-45-15 and Tetra-decagonal-60-45-30 tubes.	175

Figure 6.20 Comparing deformation mode result of mathematical against simulation result at 'Phase 1', 'Phase 2' and 'Phase 3' of symmetric tetra-decagonal tubes 179

Figure 6.21 Comparing mathematical against simulation results of force vs deformation/total height relationship of symmetric tetra-decagonal tubes of $\theta_1 = 60^\circ$, $\theta_2 = 45^\circ$ and Various θ_3 (a) 15° and (b) 30° . 182

LIST OF ABBREVIATIONS

θ_i	-	The angle between the oblique side and the vertical axis at phase- i
δ	-	The displacement.
κ	-	The bending curvature
κ_e	-	The maximum elastic curvature
ν	-	Poisson's Ratio
σ	-	Stress (N/m ²)
σ_Y	-	Yield stress (N/m ²)
σ_{UTS}	-	Ultimate stress (N/m ²)
ϵ	-	No. of element
\mathbb{Z}	-	Integers
ϵ	-	Normal strain (mm)
ϵ_y	-	Yield strain (mm)
ϵ_f	-	Fracture strain (mm)
E	-	Young's modulus (N/m ²)
E_p	-	Hardening modulus (N/m ²)
E_{in}	-	Input energy / external energy (kJ)
W^e	-	Elastic strain energy (kJ)
D	-	Plastic strain energy (kJ)
F	-	Force (N)
F^o	-	Lower bound of the actual limit loads (N)
F^*	-	Upper bound of the actual limit loads (N)
F_s	-	Actual limit loads (N)
H_i	-	Vertical height of the oblique side at phase- i , (mm)
K	-	Material constants
L	-	Length (m)
M	-	Bending moment (N)
M_e	-	Maximum elastic bending moment (N)
M_p	-	The fully plastic bending moment (N)

N	-	Normal forces (N)
Y	-	The yield stress of the material (N/m ²)
U_1	-	Displacement component in the 1-direction (mm)
U_2	-	Displacement component in the 2-direction (mm)
U_3	-	Displacement component in the 3-direction (mm)
UR_1	-	Rotational displacement component about the 1-direction
UR_2	-	Rotational displacement component about the 2-direction
UR_3	-	Rotational displacement component about the 3-direction
b	-	The width of the tube (mm)
h	-	The thickness of the tube (mm)
m	-	Number of phases
n	-	Number of sides
q	-	Hardening exponent

CHAPTER 1

INTRODUCTION

1.1 Background of the Research

In the modern era of lives, transportation is one of the main needs to travel from one location to another location and to deliver goods. Due to the advanced technology of the modern world, the vehicles could be produced in a massive volume. In Malaysia, the number of vehicles registered in the year of 2011 was 21,311,630 increased by more than 1 million from the year of 2010 (Royal Malaysia Police, 2012). Moreover, vehicles can also have very high speeds. There are also a lot of heavy vehicles like lorries and trucks on the road. The increasing number of vehicles with high speeds and massive weight will lead to a more severe damage to the people and environment if traffic accident occurs.

The number of people killed and injured due to the road accident is reported to be increasing year by year. World Health Organization (WHO) reported around 1.3 million people are killed in road traffic collisions worldwide every year (WHO, 2009). Furthermore, the number of injuries or disabilities is estimated between 20

and 50 million people worldwide every year. The European Union (EU) with the number of motor vehicles is nearly half of the about 500 million population reported the numbers of injuries and deaths from road accidents are 1200, and 34,500 respectively each year (European Commission, 2011). The United States of America (USA) with 309 million population and 256 million registered motorised vehicles in 2008, reported 33,808 deaths due to road accidents (National Highway Traffic Safety Administration, 2010). In Malaysia, nearly 7000 deaths and over 25,000 injuries have been reported in 2011 due to road accidents (Royal Malaysia Police, 2012). Hence, road traffic fatalities, disabilities, and injuries have become a major global public health issue. Due to these associated increases, society has become more aware and concerned for the safety aspects of transportation.

This has led researchers in the last few decades to study and develop impact protection systems to prevent and reduce the effects of collisions. These safety systems can be divided into two types i.e. active and passive safety systems (Johnson and Mamalis, 1978). The function of active safety systems is to prevent collision to happen. Some of the examples of active safety system are the application of electronic control systems to improve drivers' visibility, improved vehicle handling devices and anti-lock-braking systems (ABS). On the other hand, the function of passive safety systems is to reduce the collision effects to the vehicles and occupants by limiting the level of deceleration and dissipating the kinetic energy during impact in the controlled manner. Some of the examples of passive safety systems are the

build-in energy-absorbing devices/structures, seat belts, head restraints, shatterproof windscreen glass and airbags.

1.2 The Crashworthiness Properties and the Energy-absorption System

The crashworthiness or the response quality of a vehicle during collision or impact has become one of the important engineering studies in the designing process of vehicles. This study is important in order to improve on the crashworthiness properties of a vehicle so that crash fatalities can be reduced. Various aspects regarding crashworthiness have been reviewed by Johnson (1990). He mentioned that there are four major aspects that should be included in the crashworthiness designs of vehicles; (i) the consequences of the crash especially the damage caused towards the occupants, vehicles, cargoes and also to the environment, (ii) head injuries since the majority of vehicle accidents involve injuries to the head, (iii) the energy-absorption systems to absorb the kinetic energy during impact to reduce the crashworthy, and (iv) the fire risks with regards to the fuel combustion. Thus, more studies are needed to improve the crashworthiness properties of various types of vehicles. One of them is located under the study of the energy-absorption systems.

The energy-absorption structure should have the quality of small elastic dissipations to reduce the effect of repetitive decelerations to the occupant (Johnson and Reid, 1978). The energy-absorption structure should also have high irreversible or inelastic energy so that more kinetic energy can be dissipated. The various types

of irreversible energy include plastic deformation, viscous deformation energy, and energy dissipated by friction or fracture (Lu and Yu, 2003). For these two purposes, the peak of the reaction force of the energy-absorption structure should be as low as possible to reduce the elastic deformations and the reaction force should remain constant or almost constant to avoid extremely high rate of hindering. Since the elastic deformation needs to be as low as possible and at the same time the plastic deformation should be as high as possible in order to get high inelastic energy, the plastic displacement or the stroke should be sufficiently long and steady state manner. The other important factors in designing the energy-absorption system are stable and repeatable deformation mode from any uncertainty, light-weight, high specific energy-absorption capacity, low-cost and easy to install.

1.3 Problem Statements

Although there are an enormous number of researches on the various types of loading on metallic tubes, all the previous studies focussed on the cylindrical and square tubes. Hence, there is still a gap of knowledge regarding deformation behaviour of various types of geometrical tubes. The purpose of this research is to develop a general mathematical model of the deformation behaviours of various symmetric geometrical tubes subjected to lateral loading. In order to achieve this purpose, the deformation behaviour and the energy-absorbing performance of various geometrical tube shapes need to be determined. This research study focuses on the deformation behaviour of various symmetric geometrical tubes i.e. square,

hexagonal, octagonal, decagonal, dodecagonal and tetra-decagonal tubes under lateral compression between two flat rigid plates.

1.4 Research Objectives

The objectives of this research are as follows:

- (a) To develop and validate a general predictive mathematical model for the deformation behaviour of lateral collapse of the generalized symmetric geometrical tubes.
- (b) To evaluate the load - deformation behaviour under lateral loading of various symmetrical tubes i.e. square, symmetric hexagonal, octagonal, decagonal, dodecagonal and tetra-decagonal tubes.
- (c) To compare the energy-absorbing performance for different types of geometrical tubes.

1.5 Scope of Research

This research focuses on the development of the mathematical modelling of various symmetrical geometrical tube shapes which are compressed laterally in between two rigid flat plates. The geometrical tube shapes under this study are hexagonal, octagonal, decagonal, dodecagonal and tetra-decagonal. A generalized mathematical model of the lateral deformation of these shapes is determined and

presented. The finite element analysis (FEA) simulation of these tube shapes of various angles is performed to validate the mathematical model. The comparison is made between mathematical model and FEA methods on these shapes for their load-deformation behaviours and shape transformation at the phase transition. Then, the energy absorption performance is studied for these various shapes in which the best energy absorption structure can be determined. Before the FEA is employed to validate the mathematical model, the FEA should be validated with experimental results. For that purpose, the experiment on the square and cylindrical tubes compressed laterally in between two rigid flat plates is conducted along with the determination of their material properties. Then, the results between the experiment and FEA are compared to validate the FEA.

1.6 Layout of the Thesis

A newly mathematical model development and an investigation into the mechanical behaviour, performance and efficiency of various symmetric geometrical tubes i.e. square, symmetric hexagonal, octagonal, decagonal, dodecagonal and tetradecagonal tubes as energy-absorbing systems loaded in the lateral direction and compressed between two flat rigid plates is reported in this thesis. The symmetric geometrical tubes are uniformly loaded in the axial direction by loading the top flat rigid plate in the vertical downwards direction.

In Chapter 2, previous studies of energy-absorbing systems are reviewed. In the published literature, an extensive amount of work has been reported on two major types of energy-absorbing systems, i.e. axially and laterally compressed thin walled structures. Both systems are discussed in terms of their modes of deformation, energy-absorption and specific energy-absorption performance. Lastly, the focus is given on the fundamental of the mathematical modelling used in this study.

In Chapter 3, the methodological frame work of this research is presented. The research methodology consists of the experiment, the FEA simulation and the mathematical modelling. Then the experiment procedures for the tensile and compression test of square and cylindrical tubes are presented.

Chapter 4 covers the process of the FEA simulation method via ABAQUS software. The development of the various shapes and angles is discussed and then step by step input process of the module in the ABAQUS software in order to replicate the experimental work is presented.

The mathematical model development which becomes the main part of this research is discussed in Chapter 5. The development of the mathematical model discussion covers the symmetric square, hexagonal, octagonal, decagonal, dodecagonal and tetra-decagonal tube shapes which are compressed laterally in between two rigid flat plates. The discussion also covers the development of

generalized model to represent any symmetrical geometrical tube shapes under this lateral compression.

In Chapter 6, the results obtained from the experimental procedure, simulation and analytical model are discussed. The first part of this chapter discusses the validation of FEA simulation method based on the comparison between experimental and simulation results. Then, the results of load-deformation behaviour, shape transformation, the energy-absorption performance and the validation of the mathematical model results are presented and discussed for square and symmetric hexagonal tubes of various angles, symmetric octagonal tubes of various angles, symmetric decagonal tubes of various angles, symmetric dodecagonal tubes of various angles and symmetric tetra-decagonal tubes of various angles, respectively.

In Chapter 7, the conclusions are formulated based on the validation of the newly proposed mathematical model, the deformation behaviour and energy-absorption performance of the deformation behaviour of various symmetric geometrical tubes' shape i.e. square, symmetric hexagonal, octagonal, decagonal, dodecagonal and tetra-decagonal tubes. Then, a list of recommendations that could be carried out by future investigators in developing, enhancing and optimising symmetric geometrical tubes as energy-absorbing systems are presented.

CHAPTER 2

LITERATURE REVIEW

2.1 Introduction

In this chapter, different methodologies to determine the energy-absorption performance of different deformation mode are reviewed. A review of the previous researches regarding the metallic materials as the effective energy absorption structures has been done by Johnson and Reid (1978). The focus was given on the structures that could experience large plastic deformations under the collision speeds of around 50 m/s or 180 km/h so that it can absorb higher impact energy. In the meantime, the structures should have small elastic deformations to reduce the effect of repetitive decelerations to the occupant. However, due to several simplifications and assumptions made in the previous analytical models, theoretical analyses for large plastic deformations of structures have become less accurate. They suggested that in order to improve the predictive model, the structural plasticity approach should be applied. To make the analytical become more accurate, several factors such as the geometry effects, strain-hardening, strain-rate and various interactions

between different deformation modes such as bending and stretching have to be considered. Nevertheless, the improved analytical model integrating those effects have been developed since then and was reviewed also by Johnson and Reid (1986). Several achievements in the energy-absorbing systems such as uni-axial tension of ductile materials such as wires, strips and tubes were also included in this review paper.

The dynamic plastic deformation performance of structures was reviewed by Jones(1989). The simplifications and assumptions included in the previous analytical models on the load-deflection relation of the structural collapse mechanism had been discussed. The ‘secondary effects’ such as material elasticity, finite displacements, material strain-rate sensitivity, transverse shear, rotatory inertia and material strain-hardening were included so as to improve the analytical model. For repeated dynamic loads, it was observed that continuous strengths reduction at the initial and subsequent collisions experienced by structures under experimental tests were well predicted by the rigid-perfectly plastic theoretical analytical model. For tubular structures, there were two well-known sorts of failure; (1) the 'dynamic plastic buckling' and (2) ‘dynamic progressive buckling’. Dynamic plastic buckling was referred to as the global collapse since the buckle pattern was observed throughout the length of the tube. It was called dynamic plastic buckling because it occurred only during dynamic loading. This type of collapse happened due to two major effects i.e. inertia forces and material rate sensitivity. It was found that more wrinkles are produced by the inertia effect in the dynamic collapse compared to static

collapse. Several analytical models have been developed to envisage these phenomena but all of them were complicated. The other methods were by using finite element numerical methods but it was found that different softwares produced different results. On the other hand, dynamic progressive buckling occurred at low impact velocity where the effect of the inertial forces was small but still significant to the material rate sensitivity. The deformation mode of dynamic progressive buckling is like static collapse where it only occurred at one end of the tube as the deformations progressed.

A broad overview on the performances of energy-absorbing devices and their prospective utilisation in the aircraft industry had been published (Ezra and Fay, 1972). They have identified three categories of energy-absorbing devices; material deformation, extrusion and friction devices. The first category, material deformation was the main focus. The behaviour of the energy-absorbing device relied on their specific application and suitability. The performances of these devices can be measured by the specific energy, crush efficiency or energy efficiency.

Basically, there are two generic types of plastically deforming structures in energy-absorbing under quasi-static situations as shown by Calladine and English (1984). Under the compressive loading, the cellular material deformation can be categorized into two types of load-deflection namely Type I and Type II. Type I executes monotonically increasing, relatively 'flat plateau' static load-deflection curve whereas Type II produces high peak at the initial stage followed by an

immediate reduced curve. Basically, a Type I structure can be referred to as the lateral or axial compression of rings/tubes while a Type II structure can be referred to axial loading of two steel plates clamped at both ends or known as crooked plates and also to other thin-walled structures under axial loading such as struts, circular tubes and square tubes. The Type II is more sensitive to both strain rate and inertial effects and thus is more sensitive to changes in the impact velocity. This is due to the initial ‘straightness’ of the geometry structure of type II. The diagram of both types is illustrated in Figure 2.1 (a) and (b) and the load-displacement graph is shown in Figure 2.2.

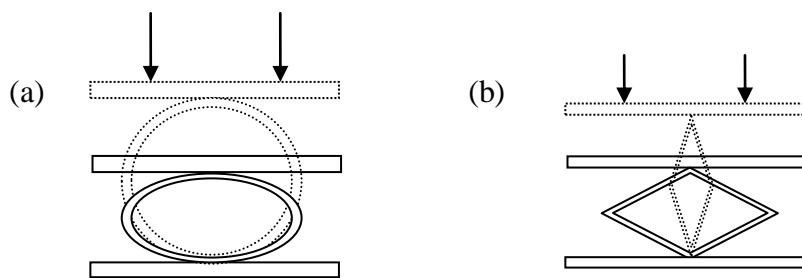


Figure 2.1: Two type of structure before (dotted line) and during compressive loading (a) Type I structure and (b) Type II structure (Calladine and English, 1984).

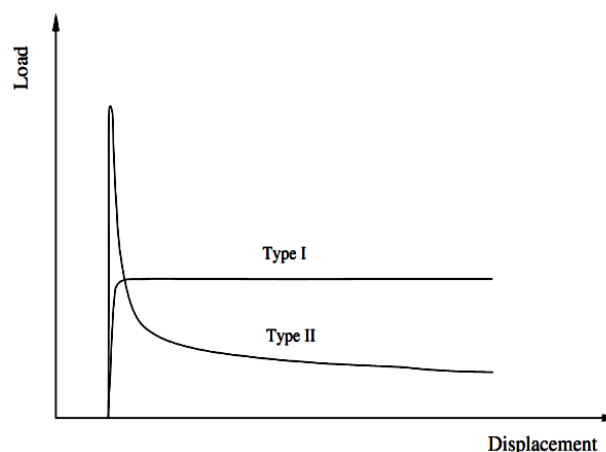


Figure 2.2: Graph of Load-Displacement of Type I and Type II (Calladine and English, 1984).

During the compression process, the cylindrical tube is deformed by undergoing three major phases which resulted in three stages in the force-deformation curve. The first stage is the linear increasing force, followed by a flat force and lastly an unbounded increasing force. The first stage is the elastic collapse, the second stage is the plastic collapse and the last stage is the densification of the cylindrical tube (Gibson and Ashby, 1997). During the plastic collapse, three types of behaviour can take place which are the strain hardening, strain softening and perfectly-plastic (Li et al., 2006), Figure 2.3 illustrates these behaviours.

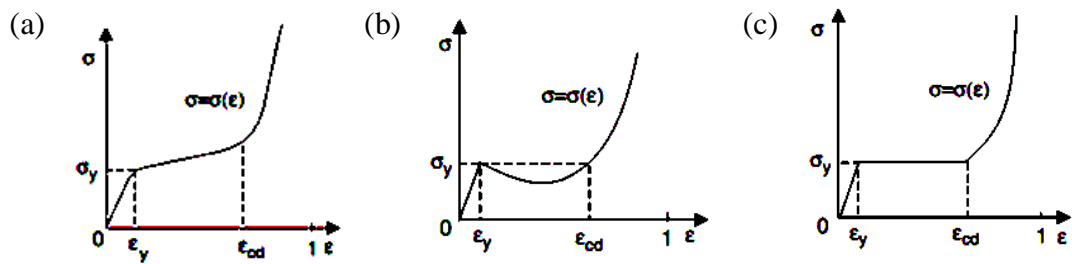


Figure 2.3: Collapse behaviour of tube under lateral compression (a) Strain-hardening behaviour, (b) Strain-softening behaviour and (c) Perfectly-plastic behaviour (Li et al., 2006).

Cellular structures comprising assemblies of simple engineering components such as tubes or rings, and bars have been used in absorbing static and dynamic forces. These components are effective impact energy absorbers because they have large plastic deformation with longer strokes which reduces decelerating forces as compared to single components (Zou et al., 2007). Furthermore, their reaction force is consistent, produces great energy-absorbing performance with recurring

deformation modes and is easy to manufacture (Lu and Yu, 2003). Basically, the study of tubular structures undergoes two key categories of loading which are along axial direction or along lateral directions. There are several methods of deformation such lateral compression, lateral indentation, axial crushing, tube splitting and tube inversion which produce different energy absorption responses. This is due to different elastic and inelastic energy dissipated by different mode during the deformation (Olabi et al., 2007). The research methodology was based mainly on experimental procedure, analytical method and simulation method that have been done by many researchers to determine the energy-absorbing capabilities of such systems.

2.2 Axial Compression

The study on the load-deflection relation of axially compressed thin cylinder was pioneered by Alexander (1960). The model was derived by equating the external work done to deform the cylinder throughout one complete collapse to the internal energy absorbed by bending and stretching at and between the joints of the complete fold. Two assumptions were made in this analytical model. The first assumption was that the cylindrical shell deformed completely outward with three hinges and circumferential stretching in of the materials in between and the second assumption was that the material had rigid-perfectly plastic behaviour. Although this model was a bit simple, it managed to show a good agreement with the experiment result. Figure 2.4 shows the deformation system produced by Alexander (1960).

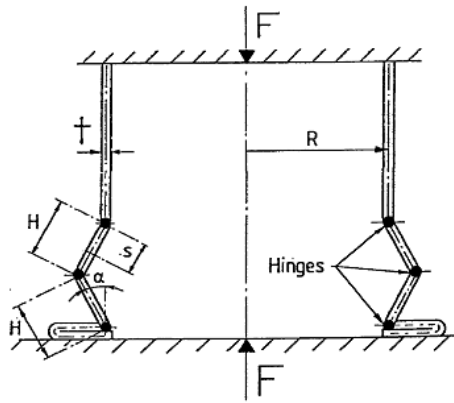


Figure 2.4: The assumption of axis-symmetric deformation mechanism (Alexander, 1960).

The improvement of model by Alexander was then presented by Johnson et al. (1977) which included a modification on the stretching energy expression. Furthermore, the improvements focused on the predictions of the deforming tube wall bends by replacing the straight line with two adhere arcs (Abramowicz and Jones, 1984a, 1986) (see Figure 2.5). The arc profile was then improved by Grzebieta (1990) (see Figure 2.6). He also adopted equilibrium approach so that the load-deflection curve can be related. Then, the eccentricity factor was introduced by Wierzbicki et al. (1992), taking account that the tube wall deforms both inward and outward (see Figure 2.7). Then, an effort was made to improve this factor by considering a global energy balance (Singace et al., 1995; Singace and Elsobky, 1996).

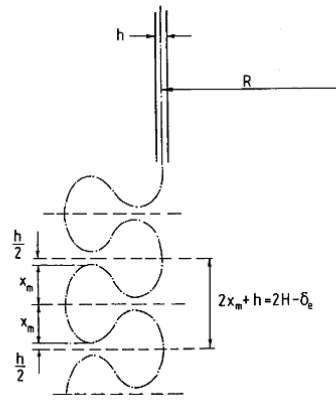


Figure 2.5: An improved axi-symmetric deformation model (Abramowicz and Jones, 1984a, 1986).

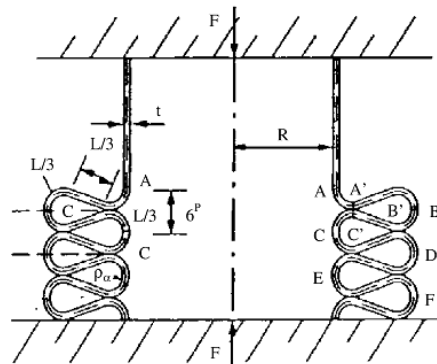


Figure 2.6: Deformation mechanism for axi-symmetric model with improved arc profile (Grzebieta, 1990).

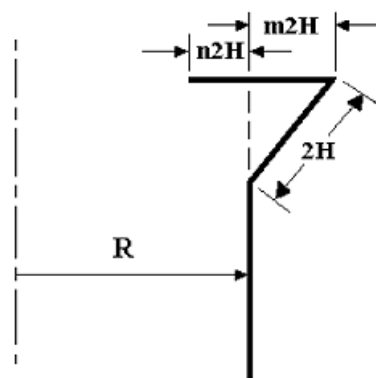


Figure 2.7: Axi-symmetric deformation model of a cylindrical tube (Wierzbicki et al., 1992).

2.2.1 Circular Tube

A detailed analysis on thin-walled circular aluminium tubes (Grade 6060) under the quasi-static axial compression had been performed by Guillow et al. (2001). The aluminium tubes were heat treated in its as-received condition with D/t ratios between $10 \leq D/t \leq 450$ and $L/D \leq 10$. A chart was made to categorize the deformation behaviour of various tube sizes. Next, the relationship between the average force and D/t ratios was empirically determined where it was found that the average force divided by the plastic bending moment, F_{AV}/M_P was equivalent to the power 0.32 of D/t and this relationship was appropriate for axisymmetric, non-symmetric and mixed modes of deformation type (refer to Figure 2.8). The axisymmetrical mode is also known as the ring mode or concertina mode and meanwhile the non-symmetrical mode is also known as diamond mode.

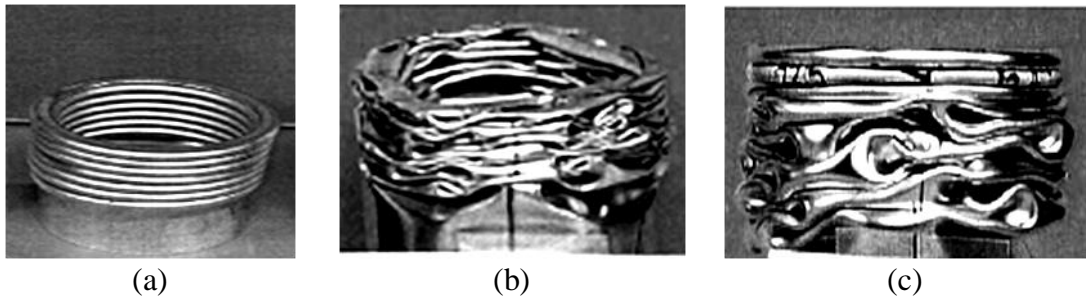


Figure 2.8: Various collapse modes for thin-walled circular aluminium tubes under axial loading (a) axisymmetric mode (concertina); (b) non-symmetric mode (diamond) and (c) mixed mode (Guillow et al., 2001)

A new type of kagome honeycomb sandwich bitubal circular column was introduced to increase the plastic deformation zones and improve the energy absorption efficiency (Zhang et al., 2010). The tube's newly designed structure consisted of two circular aluminium tubes which was filled with kagome lattice shaped cells (see Figure 2.9). A numerical method was utilised to study several properties of the composite structure such as the interaction effect, deformation mode and energy absorption capacity. It was observed that during the collapse mode, the kagome lattices buckled first causing the outer and inner skin tubes to fold locally and enhanced the plastic deformation region. The application of double layer tubes had reinforced the buckling capacity of kagome cell. In addition, the collapse of the honeycomb cell was being delayed by the wrinkled mechanism of the tube walls which intruded into the gap of the honeycomb cell. Hence, the contact effects between the honeycomb and column walls had significantly enhanced the energy absorption efficiency.

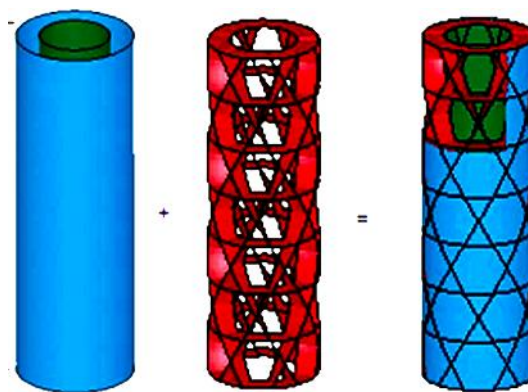


Figure 2.9: The kagome sandwich column's geometrical construction (Zhang et al., 2010).

Eyvazian et al. (2014) analyzed experimentally on the deformation behaviour, energy-absorption performance, and failure mode of corrugated cylindrical aluminium tubes under axial compressive loading. There were five corrugated geometrical shapes with different sizes and directions. They found out that, corrugated tubes produced a uniform load–displacement curve without any initial peak load. Furthermore, by using the corrugated tubes, the failure mode was found to be more predictable and controllable. Thus, it could improve the crashworthiness characteristics, controllability and collapse modes of circular tubes under axial loading.

2.2.2 Square Tube

Fyllingen et al. (2012) made an experimental study on the transition from progressive buckling to global bending during axial crushing of long square tubes. The study was performed on aluminium alloy 6060 T6 tubes with the thickness and outer width of 2.5 mm and 80 mm respectively. The impact tests were carried out in a pendulum accelerator on square tubes with lengths of 1300, 1600 and 1900 mm. The bottom ends of the tubes were fixed at the distal end to a rigid wall and the top ends of the tubes were set free. The force with the mass of 1400 kg at an initial velocity of 13 m/s was applied on the top ends of the tubes. They observed that for all the tubes, progressive buckling was initiated from the bottom towards the top of the tubes. There were two deformation modes i.e. progressive buckling and transition

from progressive buckling to global bending. They found that the longer tubes would be deformed by the latter mode. The odd behaviour development which was associated to the deformation behaviour at the fixed end had effected the transition progressive buckling to global bending. It was also found that the deformation behaviour was slowly transformed from the progressive mode to the mixed mode for the large range of tube lengths. Figure 2.10 shows the different deformation modes of long square tubes.

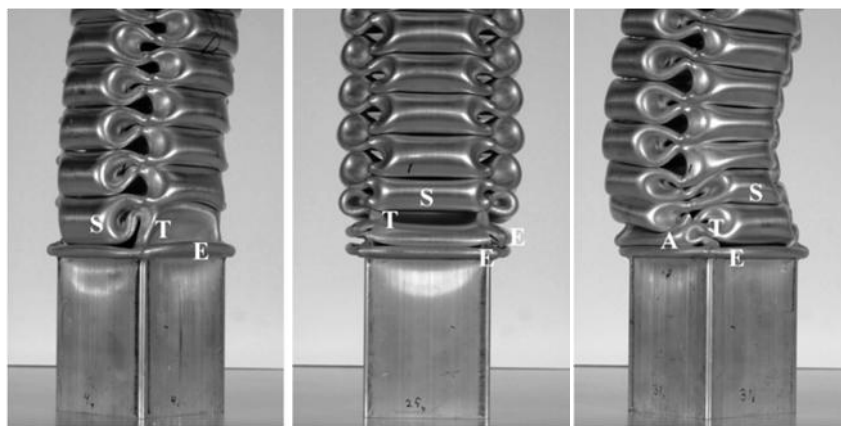


Figure 2.10: Deformation modes of square tube from left to right : One extensional lobe; Two extensional lobes and One extensional lobe and one asymmetric lobe where S = symmetric, E = extensional, A = asymmetric, T =transition (Fyllingen et al., 2012).

The energy absorption performance of longitudinally grooved square tubes subjected to axial compression has been investigated by Zhang and Huh (2009) by using the finite element analysis simulation software i.e. LS-DYNA. The walls of the square tubes were stamped to form the grooves (see Figure 2.11). The authors studied the distributions of the effective plastic strain and the thickness variations

from the stamping process. They also studied the influence of several parameters such as the width of the tube, the length of the groove and the number of the grooves, and the features of the deformation modes of grooved tubes. Based on the simulation analyses, the authors discovered that the longitudinally grooved square tubes increased 82.7% of the specific energy absorption of conventional square tubes and reduced 22.3% of the peak force of the conventional tubes. This study had also discovered that the crashworthiness of thin-walled structures could be improved by the introduction of grooves to the wall of the square tubes.

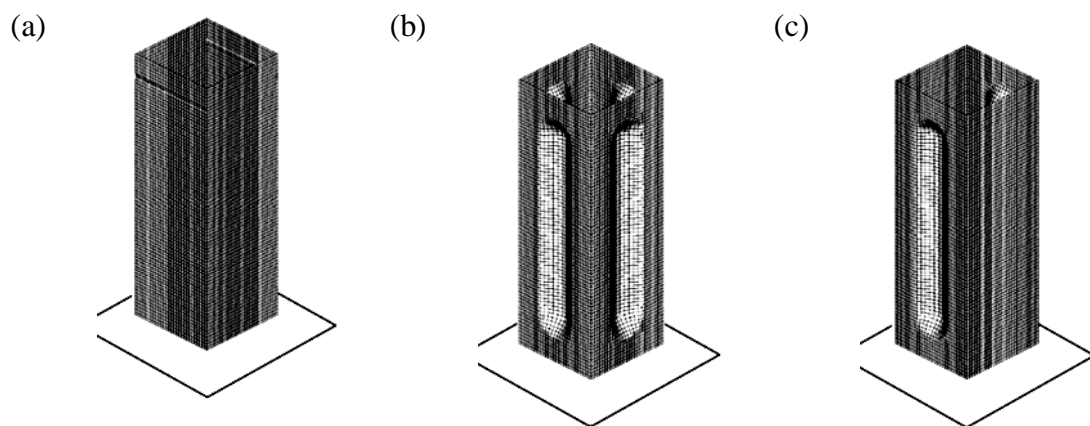


Figure 2.11: Finite element models of three types of tube: (a) conventional tube without groove; (b) tube with four grooves i.e. one groove on every sidewall; and (c) tube with grooves i.e. one groove on two opposite sidewalls (Zhang and Huh, 2009).

In order to reduce the initial peak and the subsequent fluctuations in the load-deflection curve, Song et al. (2012) introduced the origami patterns to thin-walled tubes of various cross-sectional shapes such as square, hexagon and octagon. Figure 2.12 shows the example of the origami pattern on a square cross-sections thin-walled

tube. Tubes with origami patterns were analysed through finite element analysis method. From these analyses, it was found out that the origami patterned tubes exhibited a lower initial peak force and more uniform crushing load than the existing conventional tube. Parametric studies were performed and they demonstrated the relationship between the pre-folding angles and the initial peak force with the mean crushing force for the tubes with different cross-sections. Lastly, they fabricated the origami patterned tube prototype to carry out the experimental tests. The experimental test results showed good agreement with the numerical results which included the much lower initial peak force and a smooth crushing process.

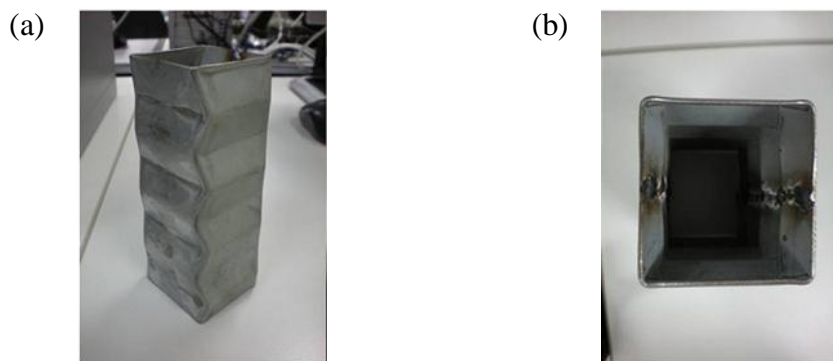


Figure 2.12: Origami pattern introduced on square tube a) side view and b) top view (Song et al., 2012).

2.2.3 Hexagonal Tube

Post-buckling behaviour of aluminium alloy extruded polygon section tubes under dynamic axial crushing has been investigated by Rossi et al. (2005). The analysis was performed explicitly by using the LS-DYNA finite element software. The analysis was divided into two stages. In the first stage, the numerical parameters and all the numerical results associated with thin-walled aluminium extruded square tubes were validated with existing published experimental data. In the second stage, the post-buckling behaviour such as extensional, symmetric and asymmetric deformation modes were examined. The numerical simulations revealed that the polygon with more number of walls or flanges had higher axial deformation load and reduced the permanent displacement parameters. For an example, hexagonal tube section increased the deformation load by 11% and reduced the permanent displacement by 10% compared to square tubes. Furthermore, the specimens with the thinnest nominal wall thickness also increased the deformation load and reduced the permanent displacement parameters by 27% and 20% respectively. Figure 2.13 illustrates the final post-buckling deformation state of a hexagonal sectioned model.

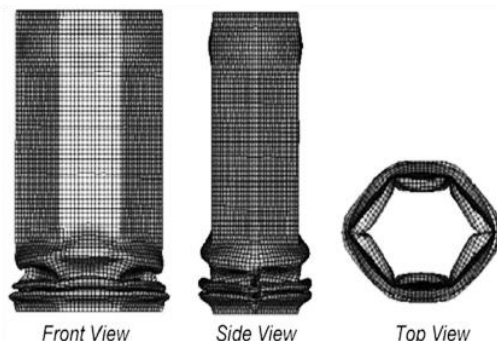


Figure 2.13: Final post-buckling deformation state of a hexagonal sectioned model using LS-DYNA (Rossi et al., 2005).

2.2.4 Frusta Tubes

The deformation mechanism and energy absorption efficiency subjected to axial quasi-static loading among a straight rectangular tubes and three tapered rectangular shapes i.e. double-tapered, triple-tapered and four or frusta tapered sides had been simulated and compared by Nagel and Thambiratnam (2005) (see Figure 2.14). This study had shown that the arrangement of the energy absorption efficiency structures from top to bottom were the triple - tapered tubes, straight tubes, frusta-tapered tubes and double-tapered tubes. Nevertheless, when the number of tapered was increased, the specific energy absorption per unit mass $\left(\frac{ea}{mass}\right)$ reduced. Hence, it was concluded that the most efficient energy absorption shape was the straight tubes if mass was considered.

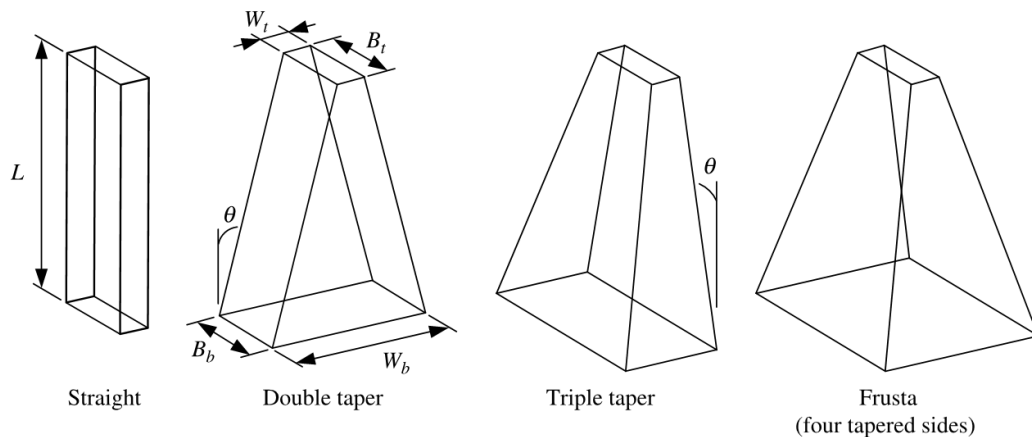


Figure 2.14: The diagram of the geometrical structure for the straight and tapered rectangular tubes (Nagel and Thambiratnam, 2005).

REFERENCES

- Abramowicz, W., & Jones, N. (1984). Dynamic axial crushing of circular tubes. *International Journal of Impact Engineering*, 2, 263–281.
- Abramowicz, W., & Jones, N. (1986). Dynamic progressive buckling of circular and square tubes. *International Journal of Impact Engineering*, 4, 243–269.
- Alexander, J. M. (1960). An approximate analysis of the collapse of thin cylindrical shells under axial loading. *Quarterly Journal Mechanics and Applied Mathematics*, 13, 10–15.
- ASTM. (2004). Designation: E 8-04. Standard test methods for tension testing of metallic materials. In *Annual Book of ASTM Standards 2004, Section 3, Metals Test Methods and Analytical Procedures, vol. 03.01, metals—mechanical testing; elevated and low-temperature tests; metallography*. ASTM, United States.
- Baroutaji, A., Morris, E., & Olabi, A. G. (2014). Thin-Walled Structures Quasi-static response and multi-objective crashworthiness optimization of oblong tube under lateral loading. *Thin Walled Structures*, 82, 262–277.
- Burton, R. H., & Craig, J. M. (1963). *An investigation into the energy absorbing properties of metal tubes loaded in the transverse direction*.
- Calladine, C. R., & English, R. W. (1984). Strain-rate and inertia effects in the collapse of two types of energy-absorbing structure. *International Journal of Mechanical Sciences*, 26(11-12), 689–701.
- De Runtz, J. A., & Hodge, P. G. (1963). Crushing of a tube between rigid plates. *Journal of Applied Mechanics*, 30, 391 – 395.
- European Commission. (2011). CARE European Road Accident Database. 19.07.11. Retrieved from http://transport/road_safety/specialist/statistics/care_reports_graphics/care_what_is_it/index_en.htm
- Eyvazian, A., Habibi, M. K., Magid, A., & Hedayati, R. (2014). Axial crushing behavior and energy absorption efficiency of corrugated tubes. *Materials and Design*, 54, 1028–1038.
- Ezra, A. E., & Fay, R. J. (1972). An assessment of energy absorbing devices for prospective use in aircraft impact situation. In G. Herman & N. Perrone (Eds.), *Dynamic response of structures* (pp. 225–246). New York: Pergamon Press.

- Fan, Z., Shen, J., & Lu, G. (2011). Investigation of Lateral Crushing of Sandwich Tubes. *Procedia Engineering*, 14, 442–449.
- Fyllingen, Ø., Langmoen, E. C., Langseth, M., & Hopperstad, O. S. (2012). Transition from progressive buckling to global bending of square aluminium tubes. *International Journal of Impact Engineering*, 48, 24–32.
- Gibson, L. J., & Ashby, M. F. (1997). *Cellular solids: structure and properties* (pp. 175–183). Cambridge: Cambridge University Press.
- Grzebieta, R. H. (1990). An alternative method for determining the behaviour of round stock tubes subjected to axial crush loads. *Thin-Walled Structures*, 9, 66–89.
- Guillow, S. R., Lu, G., & Grzebieta, R. H. (2001). Quasi-static axial compression of thin-walled circular aluminium tubes. *International Journal of Mechanical Sciences*, 43, 2103–2123.
- Gupta, N., & Ray, P. (1998). Collapse of thin-walled empty and filled square tubes under lateral loading between rigid plates. *International Journal of Crashworthiness*, 3(3), 265–85.
- Hibbitt, Karlsson, & Sorensen. (2006). ABAQUS Analysis User's Manual. In *ABAQUS Version 6.6. USA*.
- Horath, L. (2001). *Fundamentals of materials science for technologists: properties, testing and laboratory exercises* (2nd ed.). New Jersey: Prentice Hall.
- Huang, X., Lu, G., & Yu, T. X. (2002). Energy absorption in splitting square metal tubes, 40, 153–165.
- Johnson, W. (1990). The elements of crashworthiness: scope and actuality. *Proceeding Institution of Mechanical Engineers*, 204, 255–273.
- Johnson, W., & Mamalis, A. (1978). *Crashworthiness of vehicles: an introduction to aspects of collision of motor cars, ships, aircraft and railway coaches*. London: Mechanical Engineering Publications Limited.
- Johnson, W., & Reid, S. R. (1978). Metallic Energy Dissipating Systems. *Applied Mechanics Reviews*, 31, 277–288.
- Johnson, W., & Reid, S. R. (1986). Update to 'Metallic Energy Dissipating Systems [AMR 31(1978):277-288]. *Applied Mechanics Update*, 315–319.
- Johnson, W., Reid, S. R., & Reddy, T. Y. (1977). The compression of crossed layers of thin tubes. *International Journal of Mechanical Sciences*, 19(7), 423–428.

- Johnson, W., Soden, P. D., & Al-Hassani, S. T. S. (1977). Inextensional collapse of thin-walled tubes under axial compression. *Journal of Strain Analysis*, 12, 317–330.
- Jones, N. (1989). Recent studies on the dynamic plastic behaviour of structures. *Applied Mechanics Reviews*, 42(4), 95–115.
- Kim, S. C., Altenhof, W., Opperman, C. J., & Nurick, G. N. (2013). International Journal of Impact Engineering Axial splitting of circular tubes by means of blast load. *International Journal of Impact Engineering*, 53, 17–28.
- Li, Q. M., Magkiriadis, I., & Harrigan, J. J. (2006). Compressive Strain at the Onset of Densification of Cellular Solids. *Journal of Cellular Plastics*, 42, 371–392.
- Lu, G., & Yu, T. (2003). *Energy absorption of structures and materials*. Cambridge, England: Woodhead Publishing Limited.
- Mahdi, E., & Hamouda, A. M. S. (2012). Energy absorption capability of composite hexagonal ring systems. *Materials and Design*, 34, 201–210.
- Martin, J. B. (1975). *Plasticity: Fundamentals and General Problems*. Cambridge, MA: M.I.T. Press.
- Morris, E., Olabi, A. G., & Hashmi, M. S. J. (2006). Analysis of nested tube type energy absorbers with different indenters and exterior constraints. *Thin-Walled Structures*, 44(8), 872–885.
- Mutchler, L. D. (1960). Energy absorption in aluminium tubing. *Journal of Applied Mechanics*, 27, 740–743.
- Nagel, G. M., & Thambiratnam, D. P. (2005). Computer simulation and energy absorption of tapered thin-walled rectangular tubes. *Thin Walled Structures*, 43, 1225–1242.
- National Highway Traffic Safety Administration. (2010). Traffic Safety Facts 2008: A Compilation of Motor Vehicle Crash Data from the Fatality Analysis Reporting System and the General Estimates System. (Report No.: DOT HS-811–170). US Department of Transportation, Washington, DC.
- Nia, A. A., & Parsapour, M. (2014). Comparative analysis of energy absorption capacity of simple and multi-cell thin-walled tubes with triangular, square, hexagonal and octagonal sections. *Thin Walled Structures*, 74, 155–165.
- Niknejad, A., & Rahmani, D. M. (2014). Experimental and theoretical study of the lateral compression process on the empty and foam-filled hexagonal columns. *Materials and Design*, 53, 250–261.

- Olabi, A .G., Morris, E., & Hashmi, M. S. J. (2007). Metallic tube type energy absorbers : A synopsis. *Thin Walled Structures*, 45, 706–726.
- Olabi, A G, Morris, E., Hashmi, M. S. J., & Gilchrist, M. D. (2008). Optimised design of nested oblong tube energy absorbers under lateral impact loading. *Thin Walled Structures*, 35, 10–26.
- Prager, W., & Hodge, P. G. J. (1951). *Theory of Perfectly Plastics Solids*. New York: John Wiley.
- Rabinowicz, E. (1995). *Friction and wear of materials*. New York: John Wiley and Sons.
- Reddy, T. Y., & Reid, S. R. (1979). Lateral compression of tubes and tube-systems with side constraints. *International Journal of Mechanical Sciences*, 21(3), 187–199.
- Reddy, T. Y., & Reid, S. R. (1980). Phenomena associated with the crushing of metal tubes between rigid plates. *International Journal of Solids and Structures*, 16(6), 545–562.
- Reddy, T. Y., Reid, S. R., & Barr, R. (1991). Experimental investigation of inertia effects in one-dimensional metal ring systems subjected to end impact--II. Free-ended systems. *International Journal of Impact Engineering*, 11(4), 463–480.
- Redwood, R. G. (1964). Discussion on the paper by De Runtz, J. A. and Hodge Jr. P. G. (1963). *Journal of Applied Mechanics*, 31, 357–358.
- Reid, S. R., Belt, W. W., & Barr, R. A. (1983). Structural plastic shock model for one-dimensional ring systems. *International Journal of Impact Engineering*, 1(2), 175–191.
- Reid, S. R., Drew, S. L. K., & Carney, I. J. F. (1983). Energy absorbing capacities of braced metal tubes. *International Journal of Mechanical Sciences*, 25(9-10), 649–667.
- Reid, S. R., & Harrigan, J. J. (1998). Transient effects in the quasi-static and dynamic internal inversion and nosing of metal tubes, 40(2-3), 263–280.
- Reid, S. R., & Reddy, T. Y. (1978). Effect of strain hardening on the lateral compression of tubes between rigid plates. *International Journal of Solids and Structures*, 14, 213–225.
- Reid, S. R., & Reddy, T. Y. (1983). Experimental investigation of inertia effects in one-dimensional metal ring systems subjected to end impact -- I. Fixed ended systems. *International Journal of Impact Engineering*, 1(1), 85–106.

- Rossi, A., Fawaz, Z., & Behdinin, K. (2005). Numerical simulation of the axial collapse of thin-walled polygonal section tubes. *J Thin-Walled Struct*, 43(10), 1646–1661.
- Royal Malaysia Police. (2012). *Laporan perangkaan kemalangan jalan raya Malaysia 2011*. Ed. Kuala Lumpur, Malaysia.
- Shim, V. P. W., & Stronge, W. J. (1986). Lateral crushing in tightly packed arrays of thin-walled metal tubes. *International Journal of Mechanical Sciences*, 28(10), 709–728.
- Singace, A. A., & Elsobky, H. (1996). Further experimental investigation on the eccentricity factor in the progressive crushing of tubes. *International Journal of Solids and Structures*, 33, 3517–3538.
- Singace, A. A., Elsobky, H., & Reddy, T. Y. (1995). On the eccentricity factor in the progressive crushing of tubes. *International Journal of Solids and Structures*, 32, 3589–3602.
- Song, J., Chen, Y., & Lu, G. (2012). Axial crushing of thin-walled structures with origami patterns. *Thin Walled Structures*, 54, 65–71.
- WHO. (2009). *Global Status Report on Road Safety: Time for Action*. Geneva: World Health Organization.
- Wierzbicki, T., Bhat, S. U., Abramowicz, W., & Brodtkin, D. (1992). Alexander revisited - A two folding element model of progressive crushing of tubes. *International Journal of Solids and Structures*, 29, 3269–3288.
- Wu, L., & Carney, J. F. (1997). Initial collapse of braced elliptical tubes under lateral compression. *International Journal of Mechanical Sciences*, 39(9), 1023–1036.
- Wu, L., & Carney, J. F. (1998). Experimental analyses of collapse behaviours of braced elliptical tubes under lateral compression. *International Journal of Mechanical Sciences*, 40(8), 761–777.
- Yu, T. X., & Zhang, L. C. (1996). *Plastic Bending: Theory and Applications*. Singapore: World Scientific.
- Zhang, X., & Huh, H. (2009). Energy absorption of longitudinally grooved square tubes under axial compression. *Thin Walled Structures*, 47(12), 1469–1477.
- Zhang, Z., Liu, S., & Tang, Z. (2010). Crashworthiness investigation of kagome honeycomb sandwich cylindrical column under axial crushing loads. *Thin Walled Structures*, 48(1), 9–18.